

1 **Validation of MODIS 3 km Land Aerosol Optical Depth from NASA's EOS Terra and Aqua**  
2 **Missions**

3

4 Pawan Gupta<sup>1,2</sup>, Lorraine A. Remer<sup>3</sup>, Robert C. Levy<sup>2</sup>, Shana Mattoo<sup>2,4</sup>

5 [1] {Goddard Earth Sciences Technology And Research (GESTAR), Universities Space  
6 Research Association (USRA), Columbia, MD, USA}

7 [2] {NASA Goddard Space Flight Center, Greenbelt, MD 20771, USA}

8 [3] {JCET, University of Maryland – Baltimore County, Baltimore, MD 21228, USA}

9 [4] {Science Systems and Applications, Inc, Lanham, MD 20709, USA}

10 Correspondence to: Pawan Gupta (pawan.gupta@nasa.gov)

11

12 **Abstract**

13

14 In addition to the standard resolution product (10 km), The MODerate Resolution Imaging  
15 Spectroradiometer (MODIS) collection 6 (C006) data release included a higher resolution (3 km).  
16 Other than accommodations for the two different resolutions, the 10 km and 3 km Dark Target  
17 (DT) algorithms are basically the same. In this study, we perform global validation of the higher  
18 resolution Aerosol Optical Depth (AOD) over global land by comparing against Aerosol Robotic  
19 NETwork (AERONET) measurements. The MODIS-AERONET collocated data sets consist of  
20 161,410 high-confidence AOD pairs from 2000 to 2015 for MODIS-Terra and 2003 to 2015 for  
21 MODIS-Aqua. We find that 62.5% and 68.4 % of AODs retrieved from MODIS-Terra and  
22 MODIS-Aqua, respectively, fall within previously published expected error bounds of  $\pm$   
23  $(0.05+0.2 \times \text{AOD})$ , with a high correlation ( $R=0.87$ ). The scatter is not random, but exhibits a mean  
24 positive bias of  $\sim 0.06$  for Terra and  $\sim 0.03$  for Aqua. These biases for the 3 km product are  
25 approximately 0.03 larger than the biases found in similar validations of the 10 km product. The  
26 validation results for the 3 km product did not have a relationship to aerosol loading (i.e. true  
27 AOD), but did exhibit dependence on quality flags, region, viewing geometry, and aerosol spatial  
28 variability. Time series of global MODIS-AERONET differences show that validation is not static,  
29 but has changed over the course of both sensors' lifetimes, with MODIS-Terra showing more  
30 change over time. The likely cause of the change of validation over time is sensor degradation,

1 but changes in the distribution of AERONET stations and differences in the global aerosol system  
2 itself could be contributing to the temporal variability of validation.

### 3 4 **1. Introduction**

5  
6 The Moderate Resolution Imaging Spectroradiometer (MODIS) sensors, onboard the Earth  
7 Observing System (EOS) Terra and Aqua satellites, have been providing observations of Earth  
8 and the atmosphere for almost two decades (Salomonson et al., 1989). These data have been used  
9 to create a long-term set of atmospheric aerosol properties including aerosol optical depth (AOD  
10 – a measure of aerosol loading in the total atmospheric column) (Kaufman et al., 1997; Levy et  
11 al., 2013). In particular, the Dark Target (DT) algorithms applied to MODIS observations provide  
12 aerosol retrievals over both ocean and dark vegetated land surfaces (Kaufman et al., 1997, Remer  
13 et al., 2005; Levy et al., 2007a; 2007b; 2013). The DT products were designed with climate  
14 applications in mind and have been used to address a wide variety of geophysical science questions  
15 including the role of aerosols in climate-relevant processes (Kaufman et al., 2002; Christopher et  
16 al., 2002; Yu et al., 2006), cloud/precipitation modifications (Koren et al., 2009; 2012; Yuan et al.,  
17 2011; Oreopoulos et al., 2016), and long-range transport of aerosols (Kaufman et al., 2005; Yu et  
18 al., 2012). Users have even applied the DT aerosol product to address needs for monitoring,  
19 evaluating and forecasting air quality (al Saadi et al., 2005; Gupta et al., 2009; Van Donkelaar et  
20 al., 2015).

21  
22 The MODIS DT algorithm produces an aerosol product, over land and ocean, at a nominal 10 x10  
23 km<sup>2</sup> spatial resolution (referred to as “10 km” herein). This spatial resolution permits much  
24 selectivity in choosing which MODIS-measured reflectance pixels at 0.5 x 0.5 km<sup>2</sup> resolution to  
25 include in the retrieval, and generally produces smooth and accurate fields of AOD and other  
26 aerosol parameters (Remer et al., 2012). By allowing the algorithm to discard up to 90% of the  
27 available pixels and still produce a high quality aerosol product, the algorithm avoids marginal  
28 situations unfavorable for an aerosol retrieval such as cloud fringes, fragments and shadows, as  
29 well as land surfaces that do not agree with algorithm assumptions (Remer et al., 2012). The 10  
30 km product has undergone lengthy evaluation and validation, updated after each major algorithm  
31 modification (Ichoku et al., 2002; Chu et al., 2002; Remer et al., 2002, 2005; Russell et al., 2007;

1 Levy et al., 2005; 2010). Some of this evaluation was global in nature, while some local to a  
2 particular field experiment, but all concerned the 10 km MODIS DT aerosol product.

3  
4 For climate studies, the initial intention of the algorithm, 10 km spatial resolution was sufficient  
5 to characterize global and regional aerosol loading. However, as the community expanded the use  
6 of MODIS AOD to a wide variety of purposes, need arose for a finer resolution product, and a  
7 nominal 3 x 3 km<sup>2</sup> resolution (referred to as “3 km” herein) product was introduced as part of  
8 MODIS Collection 6 (Levy et al., 2013; Remer et al., 2013). The product is termed MYD04\_3K  
9 for 3 km resolution aerosol parameters derived from the MODIS-Aqua sensor and MOD04\_3K  
10 for those derived from MODIS-Terra. These products are produced operationally, over land and  
11 ocean, and the entire data records of Terra and Aqua have been reprocessed, creating a data record  
12 of almost two decades.

13  
14 Before becoming operational, Remer et al., (2013) tested the algorithm by comparing six months  
15 of global 3 km retrievals from MODIS-Aqua against available ground truth, while other  
16 independent studies (Munchak et al., 2013; Nichol and Bilal, 2016; He et al., 2017 and others)  
17 have done subsequent evaluation of the product regionally and locally. These limited comparisons  
18 suggested that the new AOD product would be sufficiently accurate to provide useful information  
19 and new perspective to the aerosol community. However, the studies also suggested that the finer  
20 resolution product might introduce additional noise and/or bias that the original coarser resolution  
21 product successfully avoided. Now that the multi-decadal 3 km product is operational and  
22 available publicly, it is time to perform a comprehensive evaluation of this finer resolution MODIS  
23 DT aerosol product. We present here the results of an analysis of a comparison of the global long-  
24 term MODIS 3 km product with collocated AEROSOL ROBOTIC NETWORK (AERONET) (Holben et  
25 al., 1998) observations.

## 26 27 **2. The MODIS dark target 3 km aerosol retrieval over land**

28  
29 The MODIS DT algorithm and products are described in detail in Levy et al., (2013) and also in  
30 the MODIS DT on-line Algorithm Theoretical Basis Document (ATBD, 2017). In summary, to  
31 retrieve aerosol parameters over land, the algorithm makes use of the reflectances measured in

1 three of MODIS' 36 spectral channels, 0.47  $\mu\text{m}$ , 0.65  $\mu\text{m}$  and 2.1  $\mu\text{m}$  (Levy et al., 2007a). These  
2 are provided in nominal spatial resolution of 0.5 x 0.5  $\text{km}^2$  (at nadir) other channels (some at 0.5  
3 x 0.5  $\text{km}^2$ , some at 1 x 1  $\text{km}^2$  resolution) are used for identifying appropriate surfaces for retrieval,  
4 and for masking clouds, snow and ice. While the 10 km standard product begins with an  
5 aggregation of 20 x 20 = 400 native-resolution pixels, the 3 km aerosol retrieval box starts with an  
6 aggregation of 6 x 6 = 36 such pixels. Native pixels are removed, as to retain only the ones most  
7 appropriate for a dark-target, over-land retrieval. Native pixels tagged as too bright for the dark  
8 target algorithm, or identified as containing cloud, surface water, snow or ice are removed from  
9 the aggregation. The remaining native pixels are sorted from darkest to brightest, and the darkest  
10 20% and brightest 50% of all remaining native pixels are removed as well. For the 3 km retrieval  
11 this means that at most 12 native pixels will remain and likely fewer. For minimum statistical  
12 robustness, the 3 km algorithm requires at least 5 native pixels (out of the initial 36). If there are  
13 insufficient native pixels (e.g. <5), output parameters are assigned fill values and no retrieval is  
14 attempted. Based on the aggregation and filtering, it is likely that there will be native pixels used  
15 by the 3 km retrieval that would have been discarded by the coarser (10 km) standard resolution  
16 product (Remer et al., 2013). The remaining native pixels are averaged, leading to a single set of  
17 spectral reflectance values that drives the aerosol retrieval. Except for downstream decisions based  
18 on number of native pixels used, the 10 km and 3 km retrievals proceed identically.

19  
20 The retrieval uses a Look Up Table (LUT) procedure in which the LUT is constructed a priori of  
21 simulated top-of-atmosphere reflectances. LUT calculations use assumptions of aerosol optical  
22 properties based on AERONET inversions (Dubovik and King, 2000) and radiative transfer. The  
23 surface reflectance is constrained by assuming an empirically based relationship between  
24 reflectance at 2.1  $\mu\text{m}$  and the reflectances at 0.65  $\mu\text{m}$  and 0.47  $\mu\text{m}$  (Levy et al., 2007a, 2007b;  
25 2013). The algorithm finds the AOD that minimizes the differences between the MODIS-observed  
26 mean spectral reflectances and the simulated reflectance values of the LUT. The primary output  
27 of the retrieval is the AOD at 0.55  $\mu\text{m}$ . Using a series of tests, the algorithm assigns a quality  
28 assurance flag (QAF) of either 3, 'good quality' or 0, 'bad quality' to the retrieval. These values  
29 can be interpreted as "confidence" in the aerosol retrieval (whether the retrieval proceeded  
30 nominally, and whether there are enough native-resolution pixels). For quantitative use of the 10  
31 km product, the MODIS DT team has recommended limiting use to retrievals designated with

1 QAF=3. In the 10 km product there must be  $\geq 51$  native pixels surviving the selection process out  
2 of a possible 120 to reach this QAF level. The similar ratio for the 3 km product is  $\geq 5$  surviving  
3 pixels out of a possible 12. Any fewer, and there is insufficient statistical information for  
4 confidence in an aerosol retrieval. Therefore, for the 3 km retrieval, a situation with fewer than 5  
5 native pixels automatically receives the designation of “poor quality” (QAF=0). For this resolution  
6 product there are no intermediate quality levels between 3 and 0 over land retrievals (Remer et al.,  
7 2013).

### 8 9 **3. Data Sets**

#### 10 11 **3.1. MODIS 3 km AOD**

12  
13 The primary data set of this study is the Collection 6 MODIS dark target retrieved aerosol optical  
14 depth at 3 km spatial resolution, derived from Terra reflectances (MOD04\_3K), or Aqua  
15 reflectances (MYD04\_3K), as described in Section 2. These are publicly available and can be  
16 downloaded from <https://ladsweb.modaps.eosdis.nasa.gov/>. Of the products in the data sets, we  
17 analyze only the AOD at 0.55  $\mu\text{m}$ .

18  
19 Applying identical algorithms to two different sensors does not guarantee identical results (Levy  
20 et al., 2015). The two MODIS DT data sets, one from MODIS-Terra and one from MODIS-Aqua  
21 must be addressed separately as individual and independent products, even though they have been  
22 created from identical algorithms with no specific tuning of parameters for each sensor. While  
23 MODIS-Terra and MODIS-Aqua began as near-identical sensors, they have evolved over their  
24 lifetimes to develop their own instrumental characteristics. For example, some detectors in Aqua’s  
25 detector array at some wavelengths have died, resulting in fewer available reflectance pixels at  
26 those wavelengths. Terra’s detector array has not lost any detectors. At the same time, we have  
27 seen drift in some of Terra’s wavelengths, resulting in measureable artificial trends in the MODIS-  
28 Terra aerosol products (Levy et al., 2013; Sayer et al., 2015; Lyapustin et al., 2014). The most  
29 flagrant of those MODIS-Terra trends have been mitigated by aggressive radiometric calibration  
30 (Toller et al., 2013), which has been applied in creating the C006 DT products. Note that some  
31 projects (e.g. Lyapustin et al., 2014; Sayer et al., 2015) have since introduced additional calibration

1 drift mitigation. However, the DT retrieval has not applied these strategies. In this work, we will  
2 analyze the C006 aerosol products from the two MODIS sensors, independently, to provide users  
3 with clear information on the strengths and limitations of each one.

### 4 5 **3.2. AERONET AOD**

6  
7 The Aerosol Robotic Network (AERONET) is NASA's global ground network of CIMEL sun-  
8 sky radiometers that make measurement of directly transmitted solar light and scattered sky light  
9 at several wavelengths during daylight hours (Holben et al., 1998). In this work, only the direct  
10 sun measurements will be used. The AERONET group processes these spectral measurements to  
11 derive AOD at the wavelengths corresponding to the direct sun measurements. The AERONET  
12 spectral AOD product is a community standard for satellite-derived AOD validation, given that  
13 AERONET's AOD uncertainty of 0.01-0.02 (Eck et al., 1999) is sufficiently more accurate and  
14 precise than can be expected by any satellite retrieval. The typical temporal frequency of direct  
15 sun measurements is every 15 minutes. The network consists of hundreds of stations, located  
16 globally, across all continents and in a wide variety of aerosol, meteorological and surface type  
17 conditions. Only stations that sufficiently represent land areas will be used here, which means we  
18 are not comparing with observations taken on small islands, ocean platforms or mobile ships.

19 The configuration of the spectral bands varies, but typically is centered at 0.34, 0.38, 0.44, 0.50,  
20 0.67, 0.87, and 1.02  $\mu\text{m}$ . Here we use a quadratic log-log fit (Eck et al., 1999) to interpolate  
21 AERONET AOD to 0.55  $\mu\text{m}$  to match the primary MODIS AOD product. AOD data from  
22 AERONET are reported for three different quality levels: unscreened (level 1.0), cloud screened  
23 (level 1.5) and cloud screened and quality assured (level 2.0). We will only use Version 2.0 Level  
24 2.0 AERONET AODs in this study.

## 25 26 **4. Spatial and Temporal Collocation**

27  
28 The validation procedure requires calculating the spatio-temporal statistics of a collocated  
29 MODIS-retrieved and AERONET-measured AOD pair (Ichoku et al. 2002; Petrenko et al., 2012;

1 Munchak et al., 2013; Remer et al., 2012). We have created a collocated data set (CDS) of AOD  
2 at 0.55  $\mu\text{m}$  from both MODIS-Terra and MODIS-Aqua, matched with AERONET, for nearly the  
3 entire mission (2003-2015 for Aqua and 2000-2015 for Terra). From here on, we use the term  
4 “pixels” to refer to the MODIS retrieval product (e.g. 3 or 10 km resolution); if referring to the  
5 native MODIS pixel resolution (e.g. 0.5 km) we will denote as “native pixel”.

6 In previous validation studies of the standard 10 km product the spatial statistics were based on  
7 groupings of either 5 x 5 MODIS product pixels ( $\sim 50 \times 50 \text{ km}^2$  box) centered on the AERONET  
8 station (Ichoku et al., 2002; Levy et al., 2010) or all the MODIS product pixels within a 27.5 km  
9 radius around the AERONET station (Petrenko et al., 2012). These spatial statistics would be  
10 matched with the temporal statistics of  $\pm 30$  minutes of AERONET observations centered at  
11 satellite overpass time. These large spatial collocation boxes will not properly test the accuracy of  
12 finer resolution satellite products to represent small-scale aerosol gradients. Therefore, Remer et  
13 al., (2013) and Munchak et al. (2013) moved to a 7.5 km radius and  $\pm 30$  minutes satellite overpass.  
14 The 7.5 km radius encompasses roughly 25 AOD pixels at nadir, which is analogous to the number  
15 of product pixels used with the coarser resolution product. In this study spatial statistics are  
16 calculated from all MODIS product pixels falling within a box of  $0.15^\circ \times 0.15^\circ$  (latitude x  
17 longitude) centered over an AERONET location. Except for Polar Regions, this is similar to a 15  
18 x 15  $\text{km}^2$  box or 7.5 km radius at nadir. Temporal statistics are calculated from all AERONET  
19 observations of AOD within  $\pm 30$  minutes of satellite overpass.

20 As recommended by the MODIS DT science team (Levy et al., 2010), unless otherwise specified,  
21 only AOD pixels with quality assurance flag ‘very good’ (QAF=3) are included in averaging over  
22 the AERONET sites. To be consistent with previous validation exercises (Levy et al., 2010), we  
23 have retained the collocated data sets only when there were at least 5 MODIS product pixels (out  
24 of a possible 25) and 2 AERONET measurements (out of a possible 2-4). The collocated data set  
25 (CDS) consists of 574 AERONET stations with 90,162 collocated pairs for MODIS-Terra and  
26 71,248 collocated pairs for MODIS-Aqua. Figure 1 shows the locations of these stations and the  
27 color-coding represents the number of collocated AERONET-MODIS AOD pairs over the station.

28 Thus, a data set (i.e. CDS) of collocated MODIS-AERONET pairs of AOD at 0.55  $\mu\text{m}$  is created  
29 that can be organized and subsampled in any number of configurations. In any subsample, or for

1 the entire data set, these ordered pairs can be plotted, one against the other to create a scatterplot,  
2 and collocation statistics calculated. We will use the following statistical parameters to quantify  
3 how well the MODIS retrievals match their collocated AERONET counterparts (Hyer et al, 2011):

- 4 • Correlation coefficient (R),
- 5 • Slope of the linear regression line,
- 6 • Root Mean Square Error (RMSE)

7 
$$\text{Mean Bias} = \frac{1}{N} \sum (\text{MODIS AOD} - \text{AERONET AOD}) \dots\dots\dots (1)$$

8 Percentage of collocations falling within expected error,

9 
$$EE = \pm(0.05 + 0.20 \times \text{AERONET AOD}) \dots\dots\dots (2)$$

10 Error Ratio (ER),

11 
$$ER = (\text{MODIS AOD} - \text{AERONET AOD})/EE \dots\dots\dots (3)$$

12 The coefficients in the EE equation were determined from evaluation of the 3 km product over the  
13 six months of Aqua data analyzed by Remer et al., (2013). Those limited results suggested that  
14 expected error bounds should be broadened to the values seen in Eq. (2) from those derived for the  
15 10 km product (EE=±[0.05+0.15 x AERONET AOD]).

16 The number of collocations (N) is another parameter used to evaluate the 3 km retrieval in the  
17 collocation data set.

18 **5. Validation Results**

19  
20 **5.1. Global Statistics**

21  
22 We first compare MODIS 3 km AOD retrievals against collocated AERONET values (Figure 2),  
23 for both the recommended ‘high quality’ retrievals (QAF=3) and for all the retrievals, regardless  
24 of quality, keeping Terra and Aqua results separate. Note that the 3 km product only tags data as

1 either ‘high quality’ or ‘low quality’. Table 1 presents the statistical parameters corresponding to  
2 this analysis while considering various combinations of QAFs.

3  
4 Globally, there is strong correlation between MODIS 3 km AOD and collocated AERONET  
5 equivalents. However, there is scatter and a positive bias to the retrievals, more so for Terra than  
6 Aqua even though the correlation is similar between the satellites. The retrieval quality identified  
7 by the algorithm corresponds well to the product accuracy as determined by collocation with  
8 AERONET observations. Algorithm-identified high quality retrievals (QAF=3) have stronger  
9 correlation, smaller RMSE and more retrievals falling within expected error than do the low quality  
10 (QAF=0) retrievals (Table 1). However, the high quality data set contains about 20% fewer  
11 retrievals than does the total data set with retrievals of all quality levels included. Figure 3 shows  
12 that the differences between Terra and Aqua in how they match AERONET values are much more  
13 apparent than the differences between QAF levels of the same satellite sensors. We note that only  
14 the high quality (QAF=3) Aqua 3 km retrievals meet expectations in terms of falling within the  
15 standard expected error bars (Remer et al., 2012; and Eq. 2).

16  
17 Table 1 also shows the corresponding validation statistics for the 10 km product for QAF=3,  
18 distinguishing between Terra and Aqua. The 10 km product, as expected, more closely matches  
19 AERONET values, having higher correlation, lower bias and RMSE, and producing more  
20 retrievals that fall within expected error bounds than does the 3 km product. We note that even in  
21 the 10 km validation statistics, mean bias for Terra is 0.03 higher than for Aqua, which is the same  
22 difference between sensors as found for the 3 km product. The results in Table 1 confirm Remer  
23 et al. (2013)’s conclusion that the 3 km product is less accurate than the standard 10 km product.  
24 The remainder of the paper will be devoted to exclusively analyzing the differences between the 3  
25 km product and AERONET, without further reference to the standard 10 km product.

## 26 27 **5.2. Regional Statistics**

28  
29 The accuracy of the 3 km AOD retrievals will be regionally and locally specific, depending on  
30 how well retrieval assumptions of surface and aerosol optical properties match actual conditions.  
31 Local cloud conditions also may introduce uncertainty into the retrieval. Furthermore, the

1 spatial/temporal variability of the area may create biases in the collocation methodology that  
2 depends on assumptions of aerosol homogeneity. Here we investigate how well the MODIS 3 km  
3 product matches AERONET over individual AERONET stations.

4  
5 For the regional and local analyses, we will use only QAF=3 retrievals and calculate the same  
6 collocation statistics for each station individually. Figure 4 plots the values for correlation  
7 coefficient, mean bias, percentage within expected error, and RMSE for each station that reported  
8 at least 100 collocations over the entire time series. In general, the MODIS 3 km retrievals show  
9 high correlations over much of the northern mid-latitudes where there are AERONET stations in  
10 abundance. Correlation is weaker at some stations in California and the arid southwest of North  
11 America, in the Caribbean, Central America, Insular SE Asia, Australia, and especially in southern  
12 South America. These are locations where the standard 10 km product also shows poor agreement  
13 with AERONET (<https://darktarget.gsfc.nasa.gov/validation/maps>). In most of these regions, like  
14 the arid southwest of North America, the surface properties do not agree with the assumptions used  
15 in the global retrieval, thereby introducing error in the retrieval.

16  
17 Not all stations with strong correlations exhibit small mean biases. For example, MODIS 3 km  
18 retrievals severely under predict AOD in the stations of west Africa, falling well below expected  
19 error there, even though those stations report high correlations with AERONET. Such a validation  
20 pattern is symptomatic of incorrect assumptions of aerosol properties. In west Africa, the interplay  
21 of heavy dust and heavy smoke, often occurring simultaneously in the atmospheric column at the  
22 same time, creates difficult situations to properly model in the aerosol retrieval. Likely the poor  
23 agreement between MODIS and AERONET there can be attributed to this difficulty. Stations in  
24 Australia, show relatively small mean biases and high percentages meeting expectations, despite  
25 poor correlations. This apparent contradiction suggests that the poor correlations are the result of  
26 small dynamic range in the scatter plots that occur when AOD is consistently low.

27  
28 In Figure 4, we see the local nature of the validation statistics. Stations in close proximity to each  
29 other sometimes report very different statistics. For example, the stations clustered across northern  
30 India, and those in an array across central South America (Brazil) range from strong positive to  
31 negative mean biases and RMSE error from 0.05 to 0.20, even though these groupings of stations

1 will fall within the same region as defined in Figure 5. This is apparent in almost any region.  
2 Some of this variability may be due to differences in the temporal extent of the AERONET record  
3 at each individual station, so that even if stations are in close proximity in space, they may actually  
4 be making measurements in entirely different years or seasons. Other differences may be related  
5 to topography, urban surfaces, or other factors. Still, the variability seen in Figure 4 shows how  
6 local conditions, and possibly the individual characteristics of the time series affect validation  
7 statistics.

8  
9 The final point to note in Figure 4 is the difference between Terra and Aqua. For example, in the  
10 mean bias plots we see how the mean bias across the North American central plains decreases  
11 from approximately positive 0.04-0.05 for Terra to slightly negative for Aqua. For many of the  
12 stations, positive mean AOD biases are higher for Terra than for Aqua. This is in agreement with  
13 the global statistics presented in Table 1.

14  
15 We next group individual stations into 17 regions, defined following Hyer et al., (2011). These  
16 are shown in Figure 5 with Table 2 presenting the regional validation statistics for each of the  
17 defined regions. We know from previous analyses presented above that there are distinctive  
18 differences between Terra and Aqua mean biases; however, in calculating the regional statistics of  
19 Table 2, we combine Terra and Aqua collocations.

20  
21 The majority of collocations are found in the northern mid-latitude regions, with E. and W.  
22 CONUS (East and West Continental United States) representing 25% of the total collocations and  
23 Europe Mediterranean and Eurasian Boreal representing another 34% of the total. MODIS 3 km  
24 retrievals from E. CONUS, Europe Mediterranean and Eurasian Boreal show very good overall  
25 agreement with AERONET, exhibiting  $R \geq 0.78$ ,  $\text{bias} \leq 0.05$  and at least 2/3 of retrievals falling  
26 within expected error. W. CONUS retrievals agree with AERONET less well, exhibiting some of  
27 the highest positive biases of any region on the globe. These four regions drive the global  
28 validation statistics, which reflect both the good agreement of E. CONUS and Europe, and the  
29 high bias of W. CONUS. Validation statistics are especially poor in Southwest Asia, where there  
30 are very few stations and collocations.

31

### 1 **5.3 Error dependencies**

2

3 We next explore the relationship between MODIS-AERONET 3 km AOD differences and various  
4 parameters for the global collocation data set. At each collocation, the AERONET AOD is  
5 subtracted from the MODIS AOD, so that a positive difference indicates a positive MODIS bias.  
6 The data is then sorted according a particular parameter in the database. Collocations are grouped  
7 into 87 bins for Terra and 67 bins for Aqua, each containing 1000 collocations. Thus, there are  
8 equal numbers of collocations in each bin, but the bins are not equally spaced along the x-axis.  
9 The mean, median and standard deviations of the MODIS-AERONET differences are calculated  
10 for each bin.

11

12 Figure 6 shows the results of this analysis as a function of AOD, both the true AOD, as measured  
13 by AERONET and the MODIS-retrieved AOD. The differences between MODIS and AERONET  
14 AOD depend very little on the true AOD. There is some suggestion of a positive-negative-positive  
15 shift of differences at the very lowest AOD ( $< 0.1$ ), but overall the differences are flat. Terra  
16 exhibits an overall positive mean bias against AERONET of about 0.06, with the bias in Aqua  
17 much less noticeable. We plot these differences against the MODIS-retrieved AOD to create a  
18 metric of retrieval accuracy that can be used to evaluate individual MODIS AOD retrievals in the  
19 absence of AERONET. Here we see a distinctive pattern between MODIS AOD bias and MODIS  
20 AOD. The higher the retrieved AOD, the greater the positive difference between MODIS and  
21 AERONET. Significant biases of  $> 0.10$  are seen for MODIS AOD values  $> 0.40$ . For retrieved  
22 AOD  $< 0.10$ , the mean differences between MODIS and AERONET are negative. This indicates  
23 that a high value of retrieved AOD has greater probability of being too high than too low, and a  
24 low value of retrieved AOD has a greater probability of being too low than too high. These results  
25 are expected, as high AOD retrievals are more sensitive to true aerosol properties whereas true  
26 surface properties become more important in low AOD retrieval.

27

28 The top row of figure 7 shows how MODIS-AERONET AOD differences vary as a function of  
29 AOD variability. Standard deviation of the retrievals in the 5x5 collocation box is a measure of  
30 the homogeneity of the aerosol across the box. The collocation methodology assumes that MODIS  
31 spatial statistics will match AERONET temporal statistics, which holds best if the aerosol field is

1 homogeneous. As variability across the box increases (i.e. STD (AOD)), we expect differences  
2 between MODIS AOD and AERONET AOD to grow. We see from Figure 7 (top row), that  
3 differences are increasingly positive as variability increases. This is because the standard deviation  
4 is not normalized, and the differences increase simply because the AOD is increasing as it does in  
5 Figure 6.

6  
7 Another test of the collocation methodology assumptions is to look for error dependencies on the  
8 number of MODIS retrievals within the 5 x 5 collocation box. Note that the methodology requires  
9 at least 5 retrievals to represent the box and may have as many as 25. We see from Figure 7  
10 (middle row) that there are dependencies. Fewer numbers of retrievals are associated with positive  
11 differences, but having almost all of the 25 retrievals available is associated with negative  
12 differences. We understand, how collocation statistics might be skewed by having fewer numbers  
13 of retrievals available to match AERONET, especially if the aerosols across the collocation box  
14 were not spatially homogeneous. Also fewer numbers of retrievals may be a result of marginal  
15 retrieval conditions caused by clouds and unfavorable surface conditions. It is less easy to  
16 understand the negative differences when the box is especially well represented with sufficient  
17 retrievals, and this require further investigation on individual situations.

18  
19 The bottom row of Figure 7 shows the MODIS-AERONET AOD differences as a function of the  
20 average number of native pixels (0.5 km) used by the MODIS 3 km retrieval in producing a value  
21 of AOD. The retrieval begins with 36 native pixels, and after masking, sorting and discarding  
22 between 5 and 12 pixels remain. The number of pixels used by the retrieval is an indication of  
23 how much masking was required. If 12 pixels remain, then no masking was required, and the  
24 situation is cloud-free and taking place over favorable surfaces. If only 5 pixels remain, there are  
25 conditions that could raise concerns. In Figure 7, we see that the fewer the pixels used by the  
26 retrieval (i.e., more masking is needed), the higher the positive bias, especially for Terra. This  
27 suggests, in the Terra retrieval, that clouds or unfavorable surface conditions are contributing to  
28 the high bias seen in the global data set. Interestingly, MODIS-AERONET differences are negative  
29 when masking is at a minimum, similar as to when the collocation box contains almost all possible  
30 retrievals. It seems that cloud-free situations with appropriate surface features are associated with

1 MODIS under predicting AERONET AOD. The same functional relationship is apparent in the  
2 Aqua data set also, but the biases, both high and low, are less pronounced.

3  
4 Figure 8 shows the MODIS-AERONET AOD differences as a function of geometry. The top row  
5 plots the differences against scattering angle, where we see positive bias increasing towards the  
6 extreme backscattering angles. The functional relationship is similar in both Terra and Aqua, but  
7 Terra's positive bias is more pronounced. The bottom row plots the differences against sensor view  
8 (i.e. zenith) angle, where the Aqua differences show little dependence on view angle, but the Terra  
9 differences increase positive biases in near nadir views. Geometrical dependencies in bias  
10 generally point to systematic inaccuracies in retrieval assumptions. These can be either in terms of  
11 surface angular functions or in aerosol optical properties. However, the difference between Terra  
12 and Aqua sensor zenith angle dependencies suggests an issue with instrument characterization,  
13 which could include geometrical functionality due to the need to calibrate across the scan mirror.

14

#### 15 **5.4 Temporal Changes**

16  
17 Examining temporal changes of validation statistics across the entire time series of the collocation  
18 database further characterizes the accuracy of the 3 km AOD product. Figure 9 plots monthly  
19 mean error ratios (Eq.3), and number of collocations for the time series of Terra (red) and Aqua  
20 (blue), separately. The error ratios (ER) compare the actual error (bias) to the expected errors (EE).  
21 The  $-1 \leq ER \leq 1$  means the actual errors are smaller than EE whereas  $|EE| > 1$ , indicates a poor  
22 match. Even if the MODIS sensors and the algorithm were entirely consistent during the time  
23 series, AERONET stations go on and off line. This causes global validation statistics to shift in  
24 local and regional emphasis, and introduces temporal variation in the global results. Therefore, we  
25 have selected 26 AERONET stations (Table 3, Figure 9) with long-term data records with  
26 consistent collocation over the entire time series for this analysis. The analysis over these selected  
27 stations allow us to examine the change in bias (and error ratios) over a longer time period without  
28 change in spatial and temporal distribution of AERONET stations. Only QAF=3 retrievals are  
29 used. During the 15 years of the collocation data set many factors have changed. For example,  
30 satellite sensor characterization is an ongoing process that employs several different measures to  
31 monitor radiometric drift, and then continuously adjusts calibration parameters to compensate for

1 that drift. Thus, even though the algorithm remains consistent throughout the data record, the  
2 inputs to that algorithm may not be, despite the best efforts of the MODIS Characterization Team.

3  
4 The time series of the monthly statistics shows strong seasonal variation of mean bias and number  
5 of collocations. Strong positive bias occurs in the April-August time period, followed by low or  
6 even negative bias in the October – February period. In addition to the seasonal variability, Figure  
7 9 also exposes long-term temporal trends. There is a steady increase of the number of collocations  
8 per month, as the AERONET network expands over time. The number of collocations nearly  
9 doubles from the early years, up and through the beginning of 2012. The last few years of the  
10 record show a decrease in collocations, in some part attributed to the lag in promoting AERONET  
11 records from Level 1.5 to Level 2.0. We only use AERONET Level 2.0 for collocations.

12  
13 The temporal mean biases for the entire time series are 0.04 and 0.014 for Terra and Aqua,  
14 respectively, corresponding to temporal mean Error Ratios (ER) of 0.55 and 0.2, respectively. The  
15 mean biases also exhibit temporal trends with biases beginning to increase around 2008/2009. The  
16 bias for Terra increased from 0.038 to 0.048 whereas these numbers for Aqua are 0.014 and 0.016.  
17 The corresponding ER increase for Terra in 2008 is from 0.48 to 0.65. The increase in ER for  
18 Aqua is negligible.

19  
20 The systematic higher biases exhibited by Terra as compared with Aqua agree with the global  
21 analysis presented above. This offset in bias between the two MODIS sensors appears systematic  
22 from the beginning of the Aqua record to the end of the time series, although the magnitude of that  
23 offset increases over time as Terra’s biases grow. The systematic greater number of collocations  
24 in the Terra data set than in Aqua’s may result from diurnal cloud patterns that create cloudier  
25 conditions in the afternoon during Aqua overpass than during Terra’s morning one. More clouds  
26 in the afternoon (King et al., 2013) may reduce the number of possible collocations. However,  
27 instrumental differences affecting available retrievals are another possibility.

## 28 29 **6. Discussion and Conclusions**

1 To validate the MODIS 3 km AOD products (MOD04\_3K and MYD04\_3K), which became  
2 publicly available in the MODIS Collection 6 release, we created a database of collocations of the  
3 product with AERONET observations. The collocation data set spanned the extent of the MODIS  
4 record from 2000 to 2015. Collocation criteria employed 0.15 x 0.15 degree latitude x longitude  
5 MODIS retrievals centered at the AERONET station and all AERONET observations  $\pm 30$  minutes  
6 of satellite overpass. Thus, the collocation box is approximately 15 km per side, for nadir views.  
7 Version 2 Level 2.0, cloud screened and quality assured AERONET observations are used, and  
8 AERONET AOD is interpolated to 0.55  $\mu\text{m}$  to match MODIS values. Overall there are over  
9 90,162 high quality collocations of Terra retrievals and over 71,248 high quality collocations for  
10 Aqua.

11  
12 The validation statistics examined include mean bias, regression slope, correlation coefficient and  
13 percentage falling within expected error bounds. In this validation exercise we hold the 3 km AOD  
14 product to expected error thresholds of  $\pm(0.05+20\%)$  (Remer et al., 2013). We find that the global  
15 3 km AOD product displays skill in matching AERONET observations with a correlation  
16 coefficient of 0.87, but there is RMSE of 0.15 and 0.13 for Terra and Aqua, respectively. The  
17 scatter is not random, but exhibits a mean positive bias of 0.06 for Terra and 0.03 for Aqua. The  
18 Remer et al. (2013) error bounds capture 2/3 of the Aqua 3 km AOD retrieval, but less than 63%  
19 of the Terra retrievals. There is significant degradation of validation accuracy if MODIS retrievals  
20 of Poor data quality (QAF=0) are included in the analysis. Thus, on a global basis we recommend  
21 using only QAF=3 MODIS 3 km retrievals for quantitative analysis. If doing so, then the expected  
22 error for the Aqua product is  $\pm(0.05 + 0.20 \times \text{AOD})$ , on a global basis, but only  $\pm(0.06 + 0.20 \times$   
23  $\text{AOD})$  for Terra, where AOD is the true AOD. However, a more accurate representation of Terra's  
24 expected error is to account for the positive bias with asymmetrical error bounds:  $-0.03 - 0.20\text{AOD}$   
25 and  $+0.13 + 0.20\text{AOD}$ . The expected error bounds contain 2/3 of all AOD retrievals. To assess the  
26 mean bias of the retrieval based on the retrieved AOD, we find that the mean bias can be modeled  
27 as  $0.19 + 0.17 \cdot \ln(\text{AOD\_MODIS} + 0.25)$  for Terra and  $0.15 + 0.14 \cdot \ln(\text{AOD\_MODIS} + 0.25)$  for  
28 Aqua. Note that mean bias itself is subject to uncertainty.

29  
30 We find a wide range of accuracy in the 3 km product locally and regionally, with spatially  
31 contiguous stations sometimes exhibiting significantly different validation statistics. The

1 distribution of validation sites is highly skewed towards the northern mid-latitudes with over 50%  
2 of all collocations in the database resulting from these areas. Within the northern mid-latitudes:  
3 Eastern North America, Europe and boreal Eurasia show some of the best agreement with  
4 AERONET. However, western North America, also in the northern mid-latitudes, exhibits some  
5 of the poorest agreement. Regions outside of the northern mid-latitudes are less well represented  
6 in the database, but we find that north/central South America including the Amazon,  
7 equatorial/southern Africa, and Australia show good agreement with AERONET. Mexico, the  
8 Caribbean, southern South America, SW Asia, East Asia, and the maritime continent of Southeast  
9 Asia generally show poor agreement. No attempt was made to isolate urban regions from rural  
10 ones, or to otherwise sort the data by surface type.

11  
12 The difference between MODIS-retrieved 3 km AOD and AERONET observed values are mostly  
13 independent of true AOD. This is unexpected as error bounds are defined as a function of the  
14 percentage of AOD  $\pm(0.05 + 0.20 \times \text{AOD})$ . However, the mean differences between MODIS 3  
15 km AOD and AERONET are dependent on AOD variability. The more variable the AOD, the  
16 higher the positive offset between MODIS and AERONET. Some of this is due to the conditions  
17 of the original MODIS retrieval, and some is due to the difficulties of a spatio-temporal match-up  
18 in the collocation methodology. We also find that the greater the need for masking clouds and  
19 unfavorable surfaces in the original retrieval, the greater the offset between MODIS and  
20 AERONET. Interesting and unexplained is the tendency for the differences between MODIS and  
21 AERONET to go negative when conditions appear to be homogeneous and cloud-free. We also  
22 find error dependencies on geometry, with greater error in the far backscattering region and for  
23 Terra only, greater error in near-nadir views. Some of these geometrical errors are introduced by  
24 uncertainties in the assumptions of surface characteristics and aerosol optical properties in the  
25 MODIS retrieval, but the difference between Terra and Aqua suggests differences in the sensors  
26 themselves.

27  
28 We continue to see differences between the sensors in how validation statistics have evolved over  
29 time. By limiting our time series analysis to only 26 AERONET stations that span the entire time  
30 series, we eliminate changes in validation statistics due to changing AERONET station  
31 distribution. We find that both sensors exhibit time series with strong seasonal dependence. Both

1 sensors have higher positive biases against AERONET in the northern spring and summer than in  
2 northern fall and winter, with Terra's positive bias always greater than Aqua's. However, during  
3 the early years of the time series, both sensors were reporting similar number of retrievals falling  
4 within expected error. This changed during 2007-2009, when Terra's accuracy began to fall off  
5 and its positive biases increased. Aqua's bias against AERONET also increased during this time  
6 frame, but not as rapidly as Terra's. While, these drifts in validation accuracy suggest changes in  
7 characterization accuracy of the MODIS sensors themselves, there are other factors. The number  
8 of collocations has fallen off towards the end of the time series. We attribute this to a lag for  
9 AERONET observations to be elevated to Level 2 status. Because of this lag, there may in fact be  
10 a change in the distribution of AERONET stations in the temporal collocation database, despite  
11 our best intentions. This may introduce a temporal trend in the validation statistics. Furthermore,  
12 the aerosol system itself has undergone significant changes since 2000, with the U.S. and Europe  
13 drastically reducing their urban/industrial emissions and substituting other types of aerosol such  
14 as wildfire smoke in the western U.S., biogenic particles during the summer in the southeastern  
15 U.S. (Hand et al., 2014; Toon et al., 2016), and transported Saharan dust around the Mediterranean  
16 (Karnieli et al., 2009). Likewise emissions and resulting AOD from other regions experience both  
17 long-term trends and interannual variability. The combination of variations in AERONET station  
18 distribution and the changing aerosol system over the time series examined may be contributing  
19 to the trends seen in the validation statistics. However, the differences between Terra and Aqua  
20 are difficult to explain without pointing to sensor characterization stability.

21  
22 The standard 10 km product that meets expected error at 67% and 74% levels for Terra and Aqua,  
23 respectively, on a global basis is measurably more accurate than the 3 km product examined here  
24 in detail. Similarly the global standard 10 km AOD product exhibits half of the mean bias with  
25 Terra and no bias at all for Aqua. These validation statistics for the 10 km standard product are  
26 preliminary. Once a more comprehensive evaluation of the Collection 6, 10 km product is  
27 completed, these validation statistics are likely to change. The 10 km product numbers are  
28 provided here only to lend perspective to our results with the finer resolution product. Given this  
29 perspective, we confirm the Remer et al. (2013) recommendation that users whose interests are  
30 global should use the more robust and accurate 10 km product, and leave the 3 km product for  
31 specific applications that require the finer resolution representation of the AOD field.

1  
2 This validation study only addressed the 3 km AOD product over land and did not evaluate the  
3 over water product. The study took a global and regional view, not a local one. Users of the  
4 product on a local level are encouraged to consider particular biases that may occur due to local  
5 conditions. For example, we know that the MODIS Collection 6 dark target AOD retrieval is  
6 systematically biased over urban surfaces (Gupta et al., 2016). This is true for both the 10 km and  
7 3 km dark target products. This problem has been addressed and is substantially mitigated with  
8 the release of the Collection 6.1 version of the algorithm (Gupta et al., 2016). In the meantime, the  
9 results here show that overall the dark target MODIS Collection 6 algorithm is producing an AOD  
10 product at 3 km resolution with sufficient accuracy and with biases well-characterized. The  
11 product can now be used quantitatively in a wide variety of science and practical applications.

12  
13

## 14 **7. Acknowledgement**

15  
16 This work was supported by the NASA ROSES program NNH13ZDA001N-TERAQEA: Terra  
17 and Aqua – Algorithms – Existing Data Products and NASA’s EOS program managed by Hal  
18 Maring. We thank MCST for their efforts to maintain and improve the radiometric quality of  
19 MODIS data, and LAADS/MODAPS for the continued processing of the MODIS products. The  
20 AERONET team (GSFC and site PIs) are thanked for the creation and continued stewardship of  
21 the sun photometer data record; which is available from <http://aeronet.gsfc.nasa.gov>.

22  
23  
24

## 23 **8. Reference**

25 Al-Saadi, J., Szykman, J., Pierce, R. B., Kittaka, C., Neil, D., Chu, D. A., Remer, L. A., Gumley,  
26 L., Prins, E., Weinstock, L., MacDonald, C., Wayland, R., Dimmick, F., and Fishman, J.:  
27 Improving national air quality forecasts with satellite aerosol observations, *Bull. Am. Meteorol.*  
28 *Soc.*, 86, 1249–1261, doi:10.1175/BAMS-86-9-1249, 2005.

29 Christopher, S. A., and Zhang, J.: Shortwave aerosol radiative forcing from MODIS and CERES  
30 observations over the oceans. *Geophysical Research Letters*, 29(18), 1859 - doi:  
31 10.1029/2002GL014803, 2002.

1 Chu, D. A., Kaufman, Y. J., Ichoku, C., Remer, L. A., Tanre, D., and Holben, B. N.: Validation of  
2 MODIS aerosol optical depth retrieval over land, *Geophys. Res. Lett.*, 29, MOD2.1–MOD2.4,  
3 doi:10.1029/2001GL013205, 2002.

4 Dubovik, O., KING, M.D.: 2000. A flexible inversion algorithm for retrieval of aerosol optical  
5 properties from Sun and sky radiance measurements *J Geophys Res*, 105(D16): 20,673-20,696,  
6 10.1029/2000JD900282, 2000.

7 Eck, T. F., Holben, B. N., Reid, J. S., Dubovik, O., Smirnov, A., O'Neill, N. T., Slutsker, I. and  
8 Kinne, S.: Wavelength dependence of the optical depth of biomass burning, urban, and desert dust  
9 aerosols, *J. Geophys. Res.*, 104, 31,333– 31,349, 1999.

10 Gupta, P., and Christopher, S. A.: Particulate matter air quality assessment using integrated  
11 surface, satellite, and meteorological products: Multiple regression approach, *J. Geophys.*  
12 *Res.*, 114, D14205, doi:10.1029/2008JD011496, 2009.

13 Gupta, P., Levy, R. C., Mattoo, S., Remer, L. A., and Munchak, L. A.: A surface reflectance  
14 scheme for retrieving aerosol optical depth over urban surfaces in MODIS Dark Target retrieval  
15 algorithm, *Atmos. Meas. Tech.*, 9, 3293-3308, <https://doi.org/10.5194/amt-9-3293-2016>, 2016.  
16

17 Hand, J. L., Schichtel, B. A., Malm, W. C., Copeland, S., Molenaar, J. V., Frank, N., and Pitchford,  
18 M.: Widespread reductions in haze across the United States from the early 1990s through 2011,  
19 *Atmos. Environ.*, 94, 671–679, doi:10.1016/j.atmosenv.2014.05.062, 2014.  
20

21 He, Qingqing & Zhang, Ming & Huang, B. T., Xuelian.: MODIS 3 km and 10 km aerosol optical  
22 depth for China: Evaluation and comparison. *Atmospheric Environment*. 153. 150-162.  
23 10.1016/j.atmosenv.2017.01.023, 2017.

24 Holben, B. N., Eck, T. F., Slutsker, I., Tanre, D., Buis, J. P., Setzer, A., Vermote, E., Reagan, J.  
25 A., Kaufman, Y. J., Nakajima, T., Lavenu, F., Jankowiak, I., and Smirnov, A.: AERONET – A  
26 federated instrument network and data archive for aerosol characterization, *Remote Sens.*  
27 *Environ.*, 66, 1–16, 1998.

1 Hsu, N.-Y. C., Jeong, M.-J. Bettenhausen, C.: Enhanced Deep Blue aerosol retrieval algorithm:  
2 The second generation, *J. Geophys. Res. Atmos.* 118 (16): 9296–9315, 10.1002/jgrd.50712, 2013.

3 Hyer, E. J., Reid, J. S., and Zhang, J.: An over-land aerosol optical depth data set for data  
4 assimilation by filtering, correction, and aggregation of MODIS Collection 5 optical depth  
5 retrievals, *Atmos. Meas. Tech.*, 4, 379–408, doi:10.5194/amt-4-379-2011, 2011.

6 Ichoku, C., D. A. Chu, S. Mattoo, Y. J. Kaufman, L. A. Remer, D. Tanré, I. Slutsker and B. N.  
7 Holben, 2002: A spatio-temporal Approach for Global Validation and Analysis of MODIS Aerosol  
8 Products. *Geophys. Res. Lett.*, 29(12), 10.1029/2001GL013205, 2002.

9 Karnieli, A., Derimian, Y., Indoitu, R., Panov, N., Levy, R. C., Remer, L. A., Maenhaut, W., and  
10 Holben, B. N.: Temporal trend in anthropogenic sulfur aerosol transport from central and eastern  
11 Europe to Israel, *J. Geophys. Res.*, 114, D00D19, doi:10.1029/2009JD011870, 2009.

12

13 Kaufman, Y. J., Gobron, N., Pinty, B., Widlowski, J., and Verstraete, M. M.: Relationship between  
14 surface reflectance in the visible and mid-IR used in MODIS aerosol algorithm – theory, *J.*  
15 *Geophys. Res.*, 29(23), 2116, doi:10.1029/2001GL014492, 2002.

16 Kaufman, Y. J., Koren, I., Remer, L. A., Tanre, D., Ginoux, P., and Fan, S.: Dust transport and  
17 deposition observed from the Terra- Moderate Resolution Imaging Spectroradiometer (MODIS)  
18 spacecraft over the Atlantic Ocean, *J. Geophys. Res.*, 110, D10S12, doi:10.1029/2003JD004436,  
19 2005.

20 Kaufman, Y. J., Tanre, D., Remer, L., Vermote, E., Chu, A., and Holben, B. N.: Operational remote  
21 sensing of tropospheric aerosol over land from EOS moderate resolution imaging  
22 spectroradiometer, *J. Geophys. Res.-Atmos.*, 102(D14), 17051– 17067, 1997.

23 King, M.D., Platnick, S.E., Menzel, W.P., Ackerman, S.A., Hubanks, P.A.: Spatial and temporal  
24 distribution of clouds observed by MODIS onboard the Terra and Aqua satellites *IEEE*  
25 *Transactions on Geoscience and Remote Sensing*, 51: 3826-3852, 2013.

26

27 Koren, I., Altaratz, O., Remer, L. A., Feingold, G., Martins, J. V. and Heiblum, R. H.: Aerosol-  
28 induced intensification of rain from the tropics to the mid-latitudes, *Nat. Geosci.*, 5(2), 118–122,  
29 doi:10.1038/ngeo1364, 2012.

1 Koren, I., Feingold, G., Jiang, H., and Altaratz, O.: Aerosol effects on the inter-cloud region of a  
2 small cumulus cloud field, *Geophys. Res. Lett.*, 36, L14805, doi:10.1029/2009GL037424, 2009.

3 Levy, R. C., Mattoo, S., Munchak, L. A., Remer, L. A., Sayer, A. M., Patadia, F., and Hsu, N. C.:  
4 The Collection 6 MODIS aerosol products over land and ocean, *Atmos. Meas. Tech.*, 6, 2989-  
5 3034, doi:10.5194/amt-6-2989-2013, 2013.

6 Levy, R. C., Munchak, L. A., Mattoo, S., Patadia, F., Remer, L. A., and Holz, R. E.: Towards a  
7 long-term global aerosol optical depth record: applying a consistent aerosol retrieval algorithm to  
8 MODIS and VIIRS-observed reflectance, *Atmos. Meas. Tech.*, 8, 4083-4110,  
9 <https://doi.org/10.5194/amt-8-4083-2015>, 2015.

10 Levy, R. C., Remer, L. A., and Dubovik, O.: Global aerosol optical properties and application to  
11 Moderate Resolution Imaging Spectroradiometer aerosol retrieval over land, *J. Geophys. Res.-*  
12 *Atmos.*, 112, D13210, doi:10.1029/2006JD007815, 2007a.

13 Levy, R. C., Remer, L. A., Kleidman, R. G., Mattoo, S., Ichoku, C., Kahn, R., and Eck, T. F.:  
14 Global evaluation of the Collection 5 MODIS dark-target aerosol products over land, *Atmos.*  
15 *Chem. Phys.*, 10, 10399–10420, doi:10.5194/acp-10-10399-2010, 2010.

16 Levy, R. C., Remer, L. A., Mattoo, S., Vermote, E. F., and Kaufman, Y. J.: Second-generation  
17 operational algorithm: retrieval of aerosol properties over land from inversion of Moderate  
18 Resolution Imaging Spectroradiometer spectral reflectance, *J. Geophys. Res.-Atmos.*, 112,  
19 D13211, doi:10.1029/2006JD007811, 2007b.

20 Levy, R.C., L.A. Remer, J.V. Martins, Y.J. Kaufman, A. Plana-Fattori, J. Redemann, P.B. Russell  
21 and B. Wenny: Evaluation of the MODIS aerosol retrievals over ocean and land during CLAMS.  
22 *J. Atmos. Sci.*, 62, 974-992, 2005.

23 Lyapustin, A., Wang, Y., Xiong, X., Meister, G., Platnick, S., Levy, R., Franz, B., Korokin, S.,  
24 Hilker, T., Tucker, J., Hall, F., Sellers, P., Wu, A., and Angal, A.: Scientific impact of MODIS C5  
25 calibration degradation and C6+ improvements, *Atmos. Meas. Tech.*, 7, 4353–4365,  
26 doi:10.5194/amt-7-4353-2014, 2014

1 Munchak, L. A., Levy, R. C., Mattoo, S., Remer, L. A., Holben, B. N., Schafer, J. S., Hostetler, C.  
2 A., and Ferrare, R. A.: MODIS 3 km aerosol product: applications over land in an urban/suburban  
3 region, *Atmos. Meas. Tech.*, 6, 1747-1759, <https://doi.org/10.5194/amt-6-1747-2013>, 2013.

4 Nichol, J. E., Bilal, M.: Validation of MODIS 3 km Resolution Aerosol Optical Depth Retrievals  
5 Over Asia. *Remote Sens.* 8, 328, 2016.

6 Oreopoulos, L., Cho, N., Lee, D., Kato, S.: Radiative effects of global MODIS cloud regimes J.  
7 *Geophys. Res. Atmos.*, 121(5): 2299–2317 [[10.1002/2015jd024502](https://doi.org/10.1002/2015jd024502)], 2016.

8 Oreopoulos, L., N. Cho, N., and Lee, D.: Using MODIS cloud regimes to sort diagnostic signals  
9 of aerosol-cloud-precipitation interactions, *J. Geophys. Res. Atmos.*, 122, 5416–5440,  
10 [doi:10.1002/2016JD026120](https://doi.org/10.1002/2016JD026120), 2017.

11 Petrenko, M., Ichoku, C., and Leptoukh, G.: Multi-sensor Aerosol Products Sampling System  
12 (MAPSS). *Atmos. Meas. Tech.*, 5, 913-926, DOI: 10.5194/amt-5-913-2012, 2012.

13 Remer, L. A., Kaufman, Y. J., Tanré, D., Mattoo, S., Chu, D. A., Martins, J. V., Li, R. R., Ichoku,  
14 C., Levy, R. C., Kleidman, R. G., Eck, T. F., Vermote, E., and Holben, B. N.: The MODIS aerosol  
15 algorithm, products, and validation, *J. Atmos. Sci.*, 62, 947–973, [doi:10.1175/JAS3385.1](https://doi.org/10.1175/JAS3385.1), 2005.

16 Remer, L. A., Mattoo, S., Levy, R. C., and Munchak, L. A.: MODIS 3 km aerosol product:  
17 algorithm and global perspective, *Atmos. Meas. Tech.*, 6, 1829-1844, [https://doi.org/10.5194/amt-](https://doi.org/10.5194/amt-6-1829-2013)  
18 [6-1829-2013](https://doi.org/10.5194/amt-6-1829-2013), 2013.

19 Remer, L. A., Mattoo, S., Levy, R. C., Heidinger, A., Pierce, R. B., and Chin, M.: Retrieving  
20 aerosol in a cloudy environment: aerosol product availability as a function of spatial resolution,  
21 *Atmos. Meas. Tech.*, 5, 1823–1840, [doi:10.5194/amt-5-1823-2012](https://doi.org/10.5194/amt-5-1823-2012), 2012.

22 Remer, L. A., Tanre, D., Kaufman, Y. J., Ichoku, C., Mattoo, S., Levy, R., Chu, D. A., Holben, B.,  
23 Dubovik, O., Smirnov, A., Martins, J. V., Li, R. R., and Ahmad, Z.: Validation of MODIS aerosol  
24 retrieval over ocean, *Geophys. Res. Lett.*, 29, MOD3.1– MOD3.4, [doi:10.1029/2001GL013204](https://doi.org/10.1029/2001GL013204),  
25 2002.

26 Russell, P. B., Livingston, J. M., Redemann, J., Schmid, B., Ramirez, S. A., Eilers, J., Kahn, R.,  
27 Chu, A., Remer, L., Quinn, P. K., Rood, M. J., and Wang, W.: Multi-gridcell validation of satellite

1 aerosol property retrievals in INTEX/ITCT/ICARTT 2004, *J. Geophys. Res.*, 112, D12S09,  
2 doi:10.1029/2006JD007606, 2007.

3 Salomonson, V. V., Barnes, W. L., Maymon, P. W., Montgomery, H. E., and Ostrow, H.: MODIS:  
4 advanced facility instrument for studies of the Earth as a system, *IEEE T. Geosci. Remote*, 27,  
5 145–153, 1989.

6 Sayer, A.M., Hsu, N.C., Bettenhausen, C., Jeong, M., Meister, G.: Effect of MODIS Terra  
7 radiometric calibration improvements on Collection 6 Deep Blue aerosol products: validation and  
8 Terra/Aqua consistency *J. Geophys. Res.*, 120, 10.1002/2015JD023878, 2015.

9 Toller, G., Xiong, X., Sun, J., Wenny, B. N., Geng, X., Kuyper, J., Angal, A., Chen, H., Madhavan,  
10 S. and Wu, A.: Terra and Aqua moderate-resolution imaging spectroradiometer collection 6 level  
11 1B algorithm, *J Appl Remote Sens*, 7, 3557, doi:10.1117/1.JRS.7.073557, 2013.

12 Toon, O. B., Maring, H., Dibb, J., Ferrare, R., Jacob, D. J., Jensen, E. J., Luo, Z. J., Mace, G. G.,  
13 Pan, L. L., Pfister, L., Rosenlof, K. H., Redemann, J., Reid, J. S., Singh, H. B., Thompson, A. M.,  
14 Yokelson, R., Minnis, P., Chen, G., Jucks, K. W., and Pszenny, A.: Planning, implementation and  
15 scientific goals of the Studies of Emissions and Atmospheric Composition, Clouds and Climate  
16 Coupling by Regional Surveys (SEAC4RS) field mission, *J. Geophys. Res.*, 121, 4967–5009,  
17 doi:10.1002/2015JD024297, 2016.

18

19 van Donkelaar, A., Martin, R. V., Brauer, M., and Boys, B. L.: Use of Satellite Observations for  
20 Long-Term Exposure Assessment of Global Concentrations of Fine Particulate Matter, *Environ.*  
21 *Health Perspect.*, 123, 135–143, doi:10.1289/ehp.1408646, 2015.

22 Yu, H., Kaufman, Y. J., Chin, M., Feingold, G., Remer, L. A., Anderson, T. L., Balkanski, Y.,  
23 Bellouin, N., Boucher, O., Christopher, S., DeCola, P., Kahn, R., Koch, D., Loeb, N., Reddy, M.  
24 S., Schulz, M., Takemura, T., and Zhou, M.: A review of measurement-based assessments of the  
25 aerosol direct radiative effect and forcing, *Atmos. Chem. Phys.*, 6, 613–666,  
26 <https://doi.org/10.5194/acp-6-613-2006>, 2006.

27 Yu, H., Remer, L., Chin, M., Bian, H., Tan, Q., Yuan, T., and Zhang, Y.: Aerosols from Overseas  
28 Rival Domestic Emissions over North America, *Science*, 337, 566–569, 2012.

1 Yuan, T., Remer, L. A., Pickering, K. E., and Yu, H.: Observational evidence of aerosol  
2 enhancement of lightning activity and convective invigoration, *Geophys. Res. Lett.*, 38, L04701,  
3 doi:10.1029/2010GL046052, 2011.

4 Yuan, T., Remer, L., and Yu, H.: Microphysical, macrophysical and radiative signatures of  
5 volcanic aerosols in trade wind cumulus observed by the A-Train, *Atmos. Chem. Phys.*, 11, 7119-  
6 7132, DOI: 10.5194/acp-11-7119-2011, 2011.

7

8

9

10

11

12

13

14

15

16

17

18

1 Table 1. Global statistics of comparison between MODIS 3 km AOD at 0.55  $\mu\text{m}$  retrievals and  
 2 collocated AERONET observations for both Terra and Aqua, corresponding to three QA  
 3 categories (QAF=0 for poor quality, QAF=0,3 for all quality and QAF=3 for high quality). The  
 4 data used for the 10km validation does not represent the same time period as 3km. MODIS-Terra  
 5 10km data period is 03/2000 to 06/2013 where as MODIS-Aqua 10km data period is 01/2003 –  
 6 06/2013.

7  
8  
9

Sensor	MODIS-Terra				MODIS-Aqua			
	3 km			10 km	3 km			10 km
Resolution								
QAF	0	0, 3	3	3	0	0, 3	3	3
<b>N</b>	18055	112210	90162	82997	13935	89804	71248	66945
<b>R</b>	0.82	0.86	0.87	0.91	0.82	0.86	0.87	0.90
<b>Bias</b>	0.052	0.061	0.059	0.03	0.021	0.031	0.027	0.00
<b>Slope</b>	1.05	1.05	1.06	1.03	0.99	1.04	1.05	1.02
<b>RMSE</b>	0.18	0.15	0.15	0.11	0.16	0.14	0.13	0.10
<b>Within EE%</b>	52.56	59.62	62.47	68.68	58.55	66.08	68.36	74.38
<b>Above EE%</b>	35.03	33.50	31.33	24.27	25.17	23.51	21.47	15.42
<b>Below EE%</b>	12.42	6.88	6.2	7.04	16.28	10.42	10.18	10.21

10  
11  
12  
13  
14  
15  
16  
17  
18  
19  
20  
21  
22  
23  
24  
25

1 Table 2. Regional statistics of inter-comparison between MODIS and AERONET. This is using  
 2 join data sets of Terra and Aqua for QAF=3 only.

3  
 4

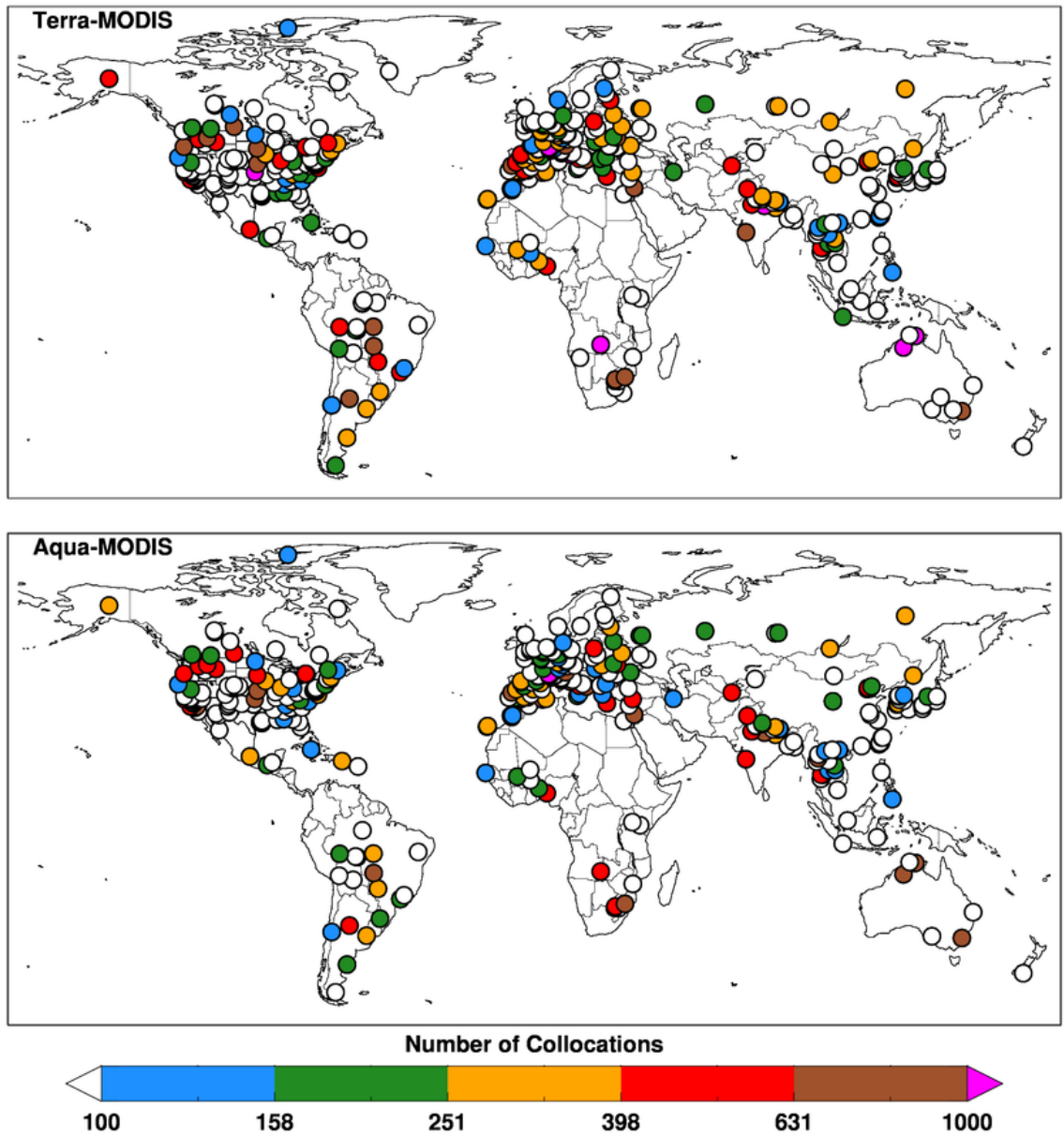
Region	N	Mean AOD	R	Bias	Slope	RMSE	Within EE%	Above EE%	Below EE%
<b>N. American Boreal</b>	4136	0.111	0.93	0.079	1.39	0.14	56.14	43.76	0.10
<b>E. CONUS</b>	22450	0.129	0.90	0.029	1.22	0.09	73.41	19.74	6.85
<b>W. CONUS</b>	17645	0.096	0.68	0.116	1.45	0.19	45.34	53.27	1.39
<b>Central America</b>	2499	0.203	0.87	0.084	1.25	0.18	51.62	40.42	7.96
<b>South America</b>	5577	0.276	0.96	-0.007	1.20	0.16	64.16	9.16	26.68
<b>S. South America</b>	5393	0.107	0.63	0.048	1.13	0.18	48.54	28.48	22.97
<b>Africa south of equator</b>	5849	0.184	0.81	-0.020	0.71	0.10	68.44	12.84	18.72
<b>Equatorial Africa</b>	270	0.203	0.90	0.002	1.03	0.08	77.78	11.85	10.37
<b>Africa north of equator</b>	9870	0.302	0.83	-0.039	0.63	0.18	61.00	18.50	20.50
<b>SW Asia</b>	405	0.220	0.78	0.164	1.25	0.21	33.58	66.17	0.25
<b>Europe - Mediterranean</b>	39792	0.162	0.79	0.043	1.06	0.11	70.62	24.63	4.75
<b>Eurasian Boreal</b>	13473	0.181	0.91	0.043	1.14	0.09	73.11	24.20	2.69
<b>East Asia Mid-Latitudes</b>	10009	0.370	0.91	0.110	1.09	0.20	56.03	41.22	2.75
<b>Peninsular Southeast Asia</b>	5259	0.501	0.91	0.039	1.05	0.18	68.09	22.02	9.89
<b>Indian Subcontinent</b>	8449	0.479	0.86	0.070	1.05	0.19	68.35	26.78	4.86
<b>Insular Southeast Asia</b>	853	0.243	0.85	0.118	1.03	0.20	50.41	48.30	1.29
<b>Australian Continent</b>	5965	0.087	0.59	-0.021	0.57	0.08	69.52	8.92	21.56

5  
 6  
 7  
 8

1 Table 3. List of selected AERONET stations for the long-term analysis as presented in figure 9.  
 2

Site Name	Latitude	Longitude
Canberra	-35.271	149.111
Skukuza	-24.992	31.587
Lake_Argyle	-16.108	128.749
CUIABA-MIRANDA	-15.729	-56.021
Mongu	-15.254	23.151
Jabiru	-12.661	132.893
Chiang_Mai_Met_Sta	18.771	98.972
Kanpur	26.513	80.232
Izana	28.309	-16.499
Saada	31.626	-8.156
Nes_Ziona	31.922	34.789
TABLE_MOUNTAIN_CA	34.380	-117.680
FORTH_CRETE	35.333	25.282
Blida	36.508	2.881
Cart_Site	36.607	-97.486
Fresno	36.782	-119.773
Evora	38.568	-7.912
GSFC	38.992	-76.840
KONZA_EDC	39.102	-96.610
XiangHe	39.754	116.962
BSRN_BAO_Boulder	40.045	-105.006
Lecce_University	40.335	18.111
Rome_Tor_Vergata	41.840	12.647
OHP_OBSERVATOIRE	43.935	5.710
Carpentras	44.083	5.058
Modena	44.632	10.945

3  
 4  
 5  
 6  
 7  
 8  
 9  
 10  
 11  
 12  
 13  
 14  
 15



1  
2  
3  
4  
5  
6  
7  
8  
9  
10  
11  
12

Figure 1. Locations of AERONET stations used in the validation study. The color scale shows the number of coincident MODIS-AERONET data points over each station for the entire period. Top panel is for MODIS-Terra and bottom panel for MODIS-Aqua. Most stations operated for only a subset of the 13 to 15 year record.

1  
2  
3  
4  
5  
6  
7  
8  
9  
10  
11  
12  
13  
14  
15  
16  
17  
18  
19  
20  
21  
22  
23  
24  
25  
26  
27  
28  
29  
30  
31  
32  
33  
34  
35  
36  
37  
38  
39  
40  
41  
42  
43  
44  
45  
46

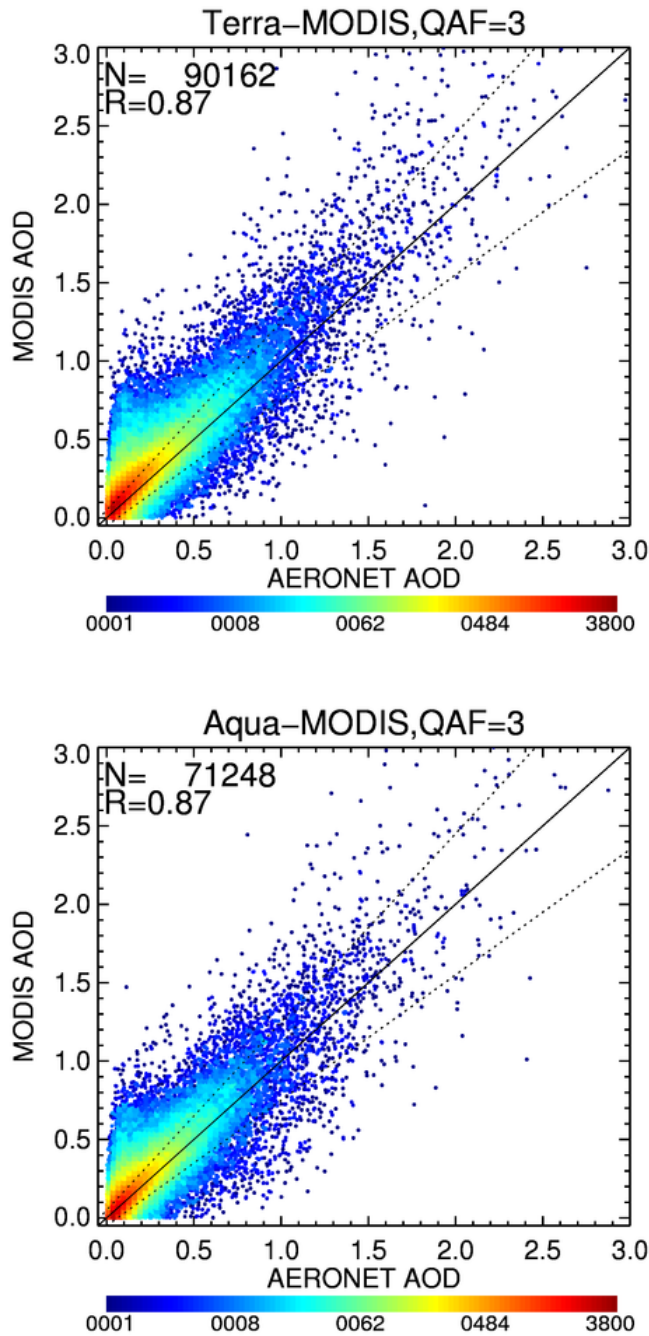
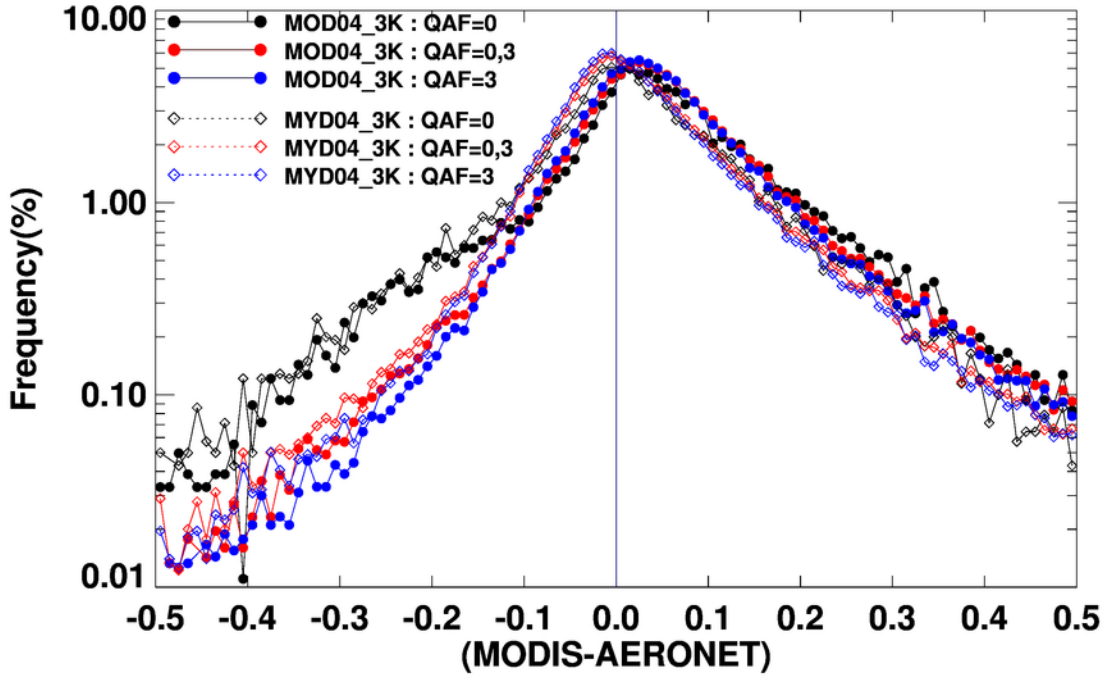


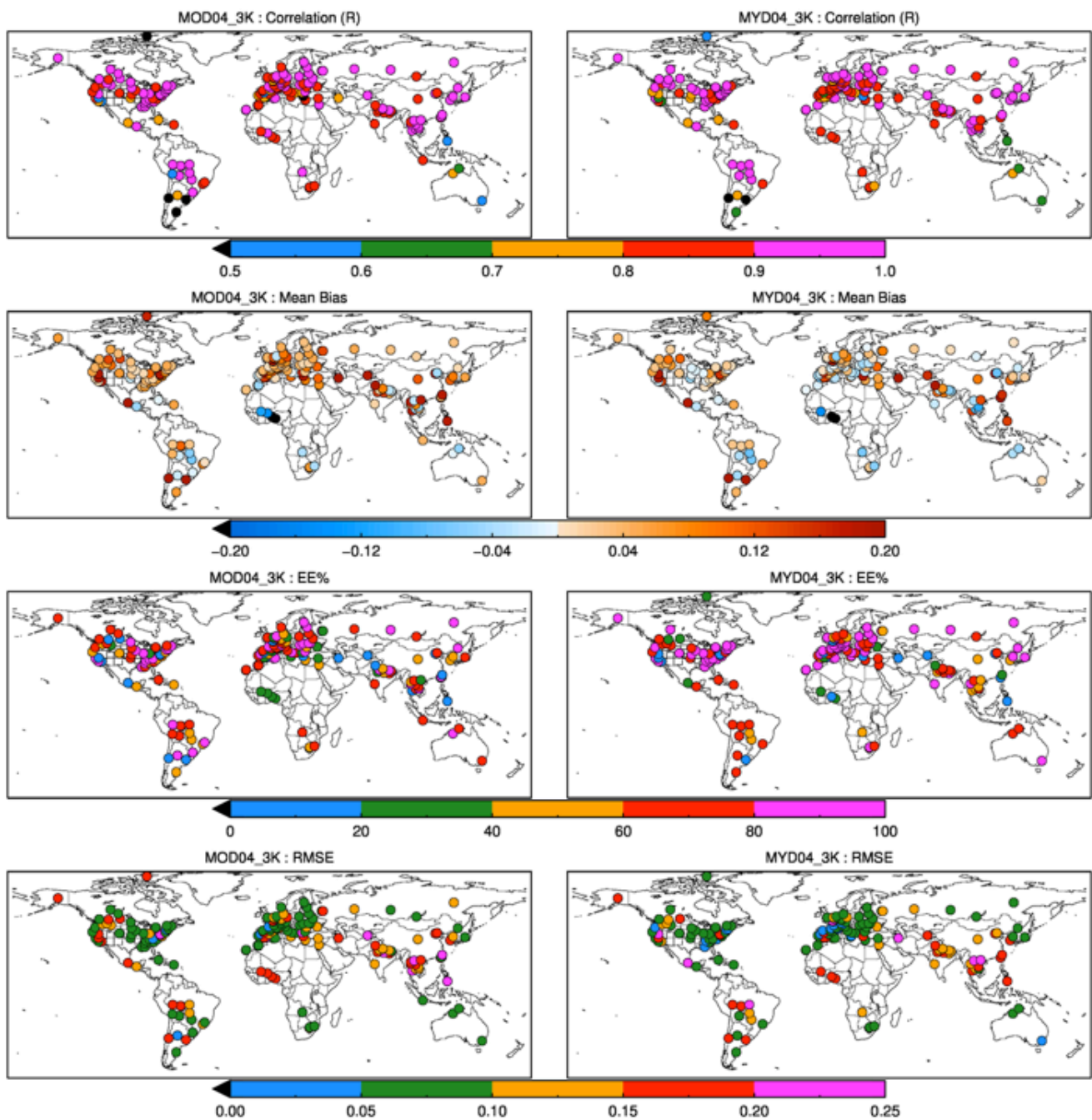
Figure 2. Two-dimensional density scatter plot of MODIS 3 km AOD versus AERONET observed AOD at 0.55  $\mu\text{m}$  for the global collocation data set. The top panel is for MODIS-Terra for only the retrievals identified as ‘high quality’ (QAF=3), and the bottom panel is for MODIS-Aqua for QAF=3. The solid line denotes the 1:1 line, and the dashed lines denote the envelope of the expected error (EE), defined by Eq. 2.

1  
2  
3



4  
5  
6  
7  
8  
9  
10  
11  
12  
13  
14  
15  
16  
17  
18  
19  
20  
21  
22  
23  
24  
25

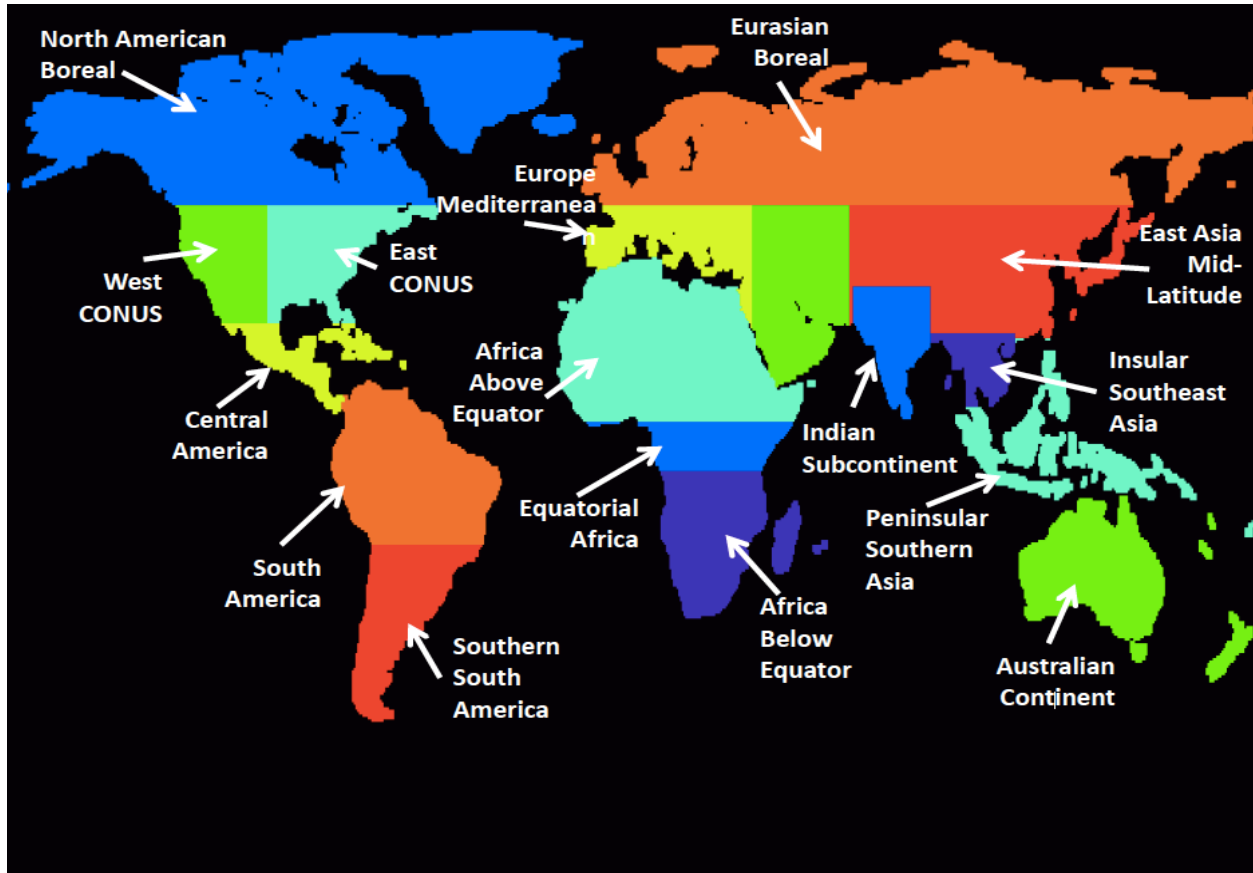
Figure 3. Global distribution of mean bias in MODIS 3 km AOD retrievals with respect to collocated AERONET observations. The circular dots with solid lines are for Terra values and diamond dots with dotted lines are for Aqua values. The colors vary for the three quality levels (QAF=0, poor quality; QAF=3, high quality; and QAF=0&3, all quality).



1  
 2 Figure 4. Statistics calculated from the collocation database at each AERONET station, individually,  
 3 for Terra on the left and Aqua on the right. Shown are values for correlation coefficient (R), mean bias,  
 4 percentage within expected error (EE%), and RMSE. Only stations with at least 100 collocations are  
 5 plotted, which may differ between the two satellites, and only collocations with MODIS retrievals of  
 6 QAF=3 are included.

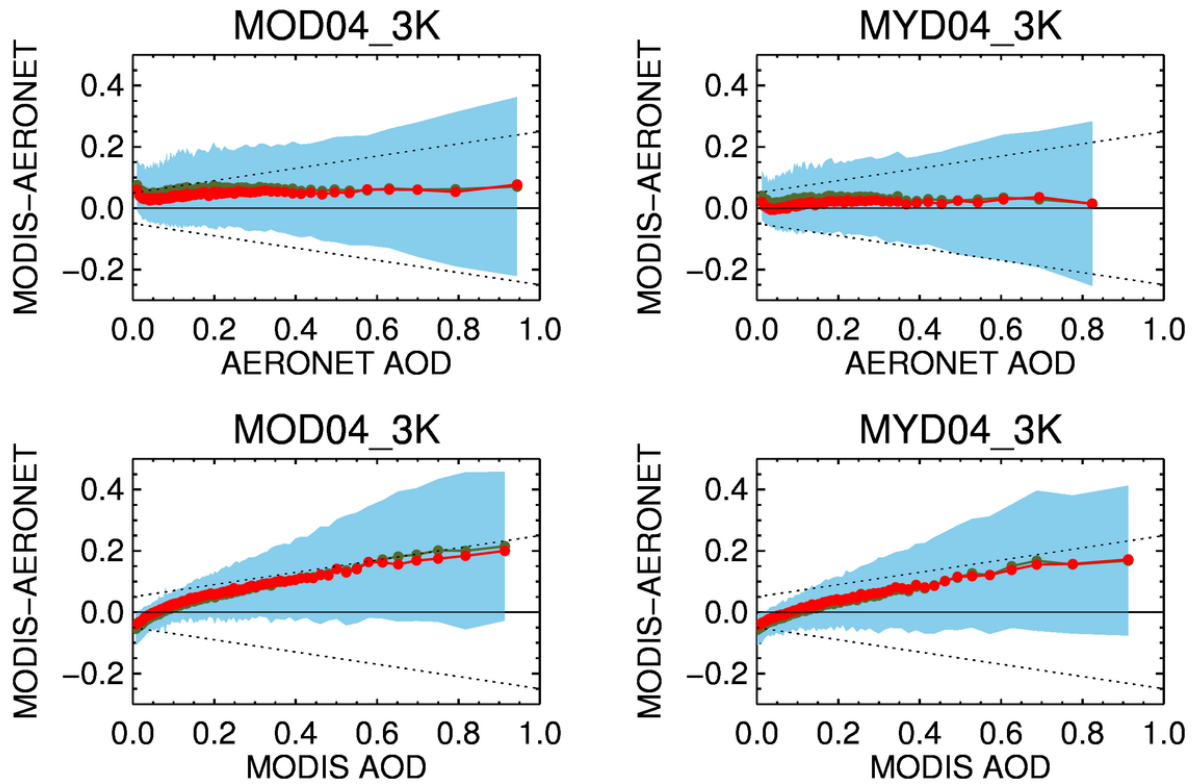
7  
 8

1



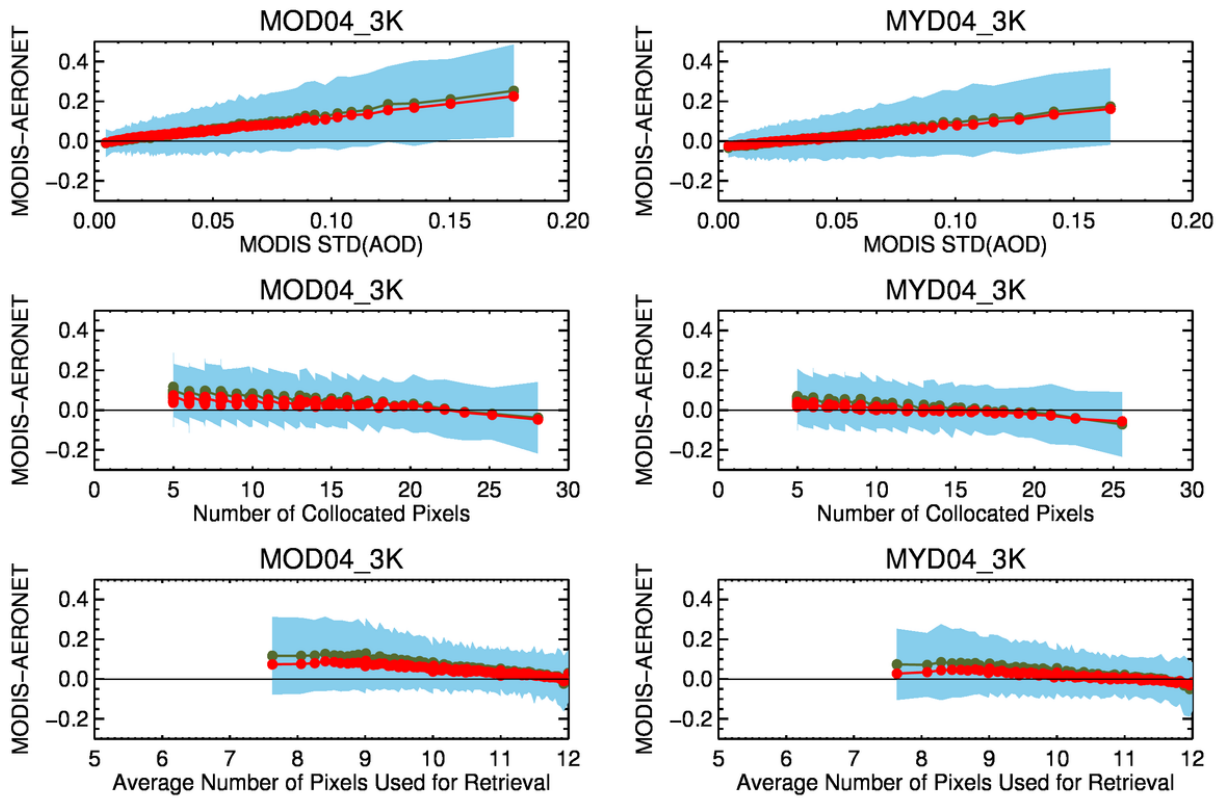
2  
3  
4  
5  
6  
7  
8  
9  
10  
11  
12  
13  
14  
15  
16  
17  
18  
19  
20  
21

Figure 5. Map showing 17 selected parts of the world where regional analysis is performed.



1  
2  
3  
4  
5  
6  
7  
8  
9  
10  
11  
12  
13  
14  
15  
16  
17  
18  
19  
20  
21  
22  
23  
24

Figure 6. AOD differences between the MODIS 3 km product and AERONET for the global collocation data set, QAF=3, as a function of AERONET AOD (top), MODIS AOD (bottom). The left column shows Terra values and the right column shows Aqua. The global data set was sorted according to AOD, binned into bins with equal number of collocations, and then mean, median and standard deviation of each bin was calculated. Red dots and line show the mean. Black dots and line show the median. The blue cloud indicates one standard deviation of each bin. The horizontal black line denotes zero difference, and the dashed lines indicate EE envelopes. Positive values indicate that MODIS AOD is higher than AERONET.



1  
2  
3  
4  
5  
6  
7  
8  
9  
10  
11  
12  
13  
14  
15  
16  
17  
18  
19  
20  
21  
22  
23  
24  
25

Figure 7. Same as Figure 6 except for standard deviation of MODIS AOD within the 5x5 collocation box (top row), number of MODIS retrievals with the 5x5 collocation box (middle row), and number of MODIS reflectance native pixels used by the retrieval, averaged for all retrievals made in the 5x5 collocation box (bottom row).

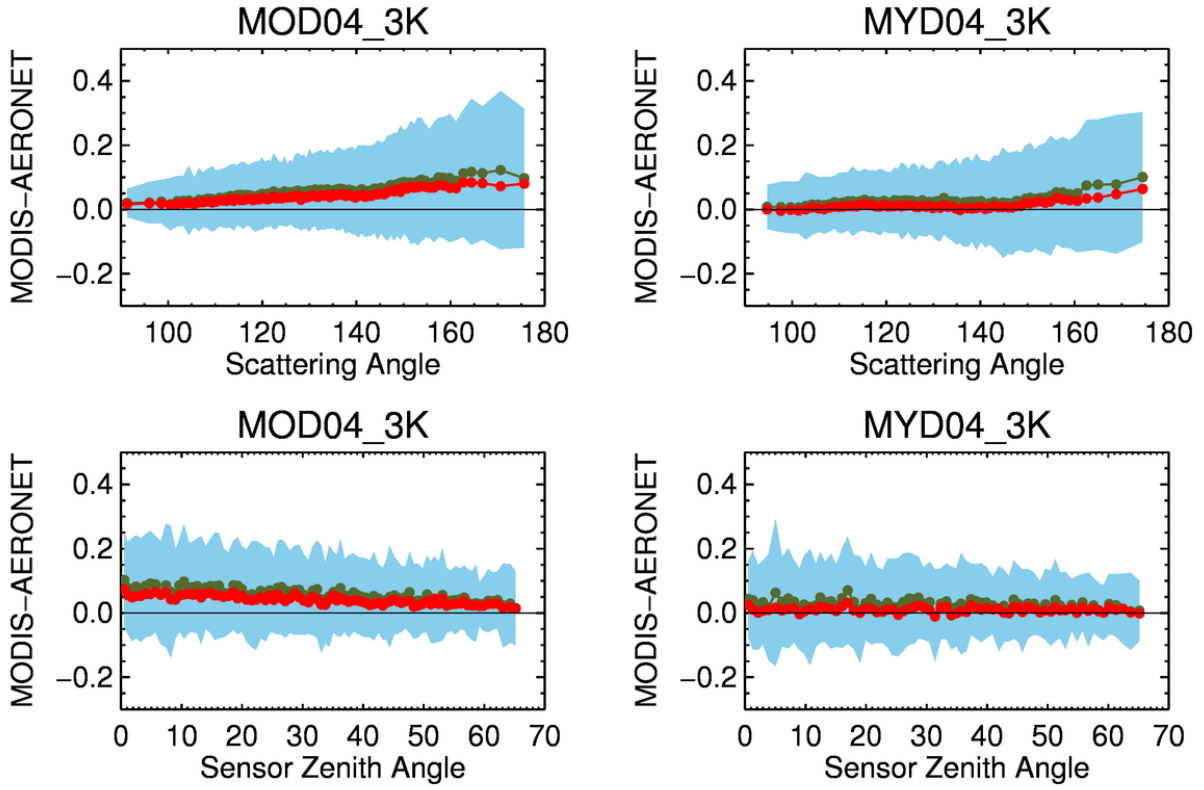
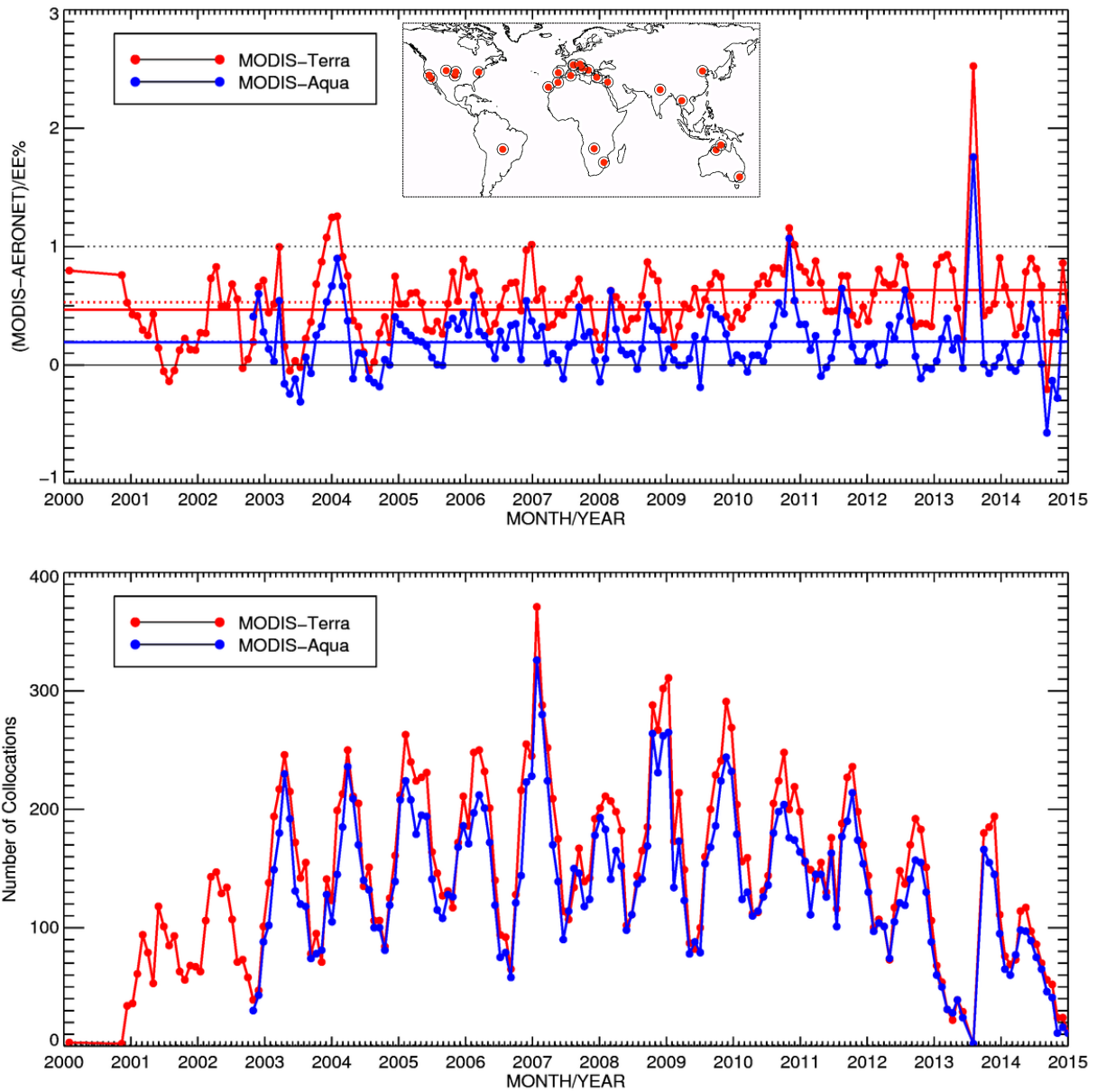


Figure 8. Same as Figure 6 except for scattering angle (top) and sensor zenith angle (bottom).

1  
2  
3  
4  
5  
6  
7  
8  
9  
10  
11  
12  
13  
14  
15  
16  
17  
18  
19  
20  
21  
22  
23  
24  
25



1  
 2  
 3 Figure 9. Time series of monthly mean error ratios (Eq. 3) (top), and number of collocations  
 4 (bottom) for the global collocation data set from 26 selected long-term AERONET stations. The  
 5 Terra record is in red, and Aqua in blue. Note Aqua's record begins two years after Terra, and the  
 6 total number of collocations is temporally variant. Only MODIS 3 km retrievals with QAF=3 are  
 7 included. The horizontal red and blue lines are temporal means of ER. Dotted red and blue  
 8 horizontal lines indicate long-term temporal mean ER for each satellite. Solid red lines are  
 9 temporal mean ER calculated for Terra for two periods (2000-2010) and (2011-2015). The map  
 10 in the inset shows locations of AERONET stations used in this analysis with more details provided  
 11 in table 3